Tracking the Galileo Spacecraft With the DSCC Galileo Telemetry Prototype

T. T. Pham and S. Shambayati
Telecommunications Systems Section

D. E. Hardi
Communications Systems Research Section

S. G. Finley
Tracking Systems and Applications Section

On day of the year (DOY) 062, 1994, a prototype of the Deep Space Communications Complex Galileo Telemetry subsystem successfully tracked and processed signals from the Galileo spacecraft, under fully suppressed-carrier modulation. The demonstration took place at Goldstone, employing the 70-m antenna and the 34-m high-efficiency antenna. This article presents the findings from that demonstration. Specific issues are the system performance in terms of signal-to-noise (SNR) degradation and the arraying gain. Validation of the test results is via symbol-error-rate measurement and the standard symbol SNR. The analysis is also extended to include characterization of the signal received from Galileo.

I. Introduction

On day of the year (DOY) 062, 1994, a prototype of the Deep Space Communications Complex (DSCC) Galileo Telemetry (DGT) subsystem successfully demonstrated signal acquisition and telemetry processing with the Galileo spacecraft. The DGT is being developed to support the Galileo mission, in response to the failure of the spacecraft X-band (8.415-GHz) high-gain antenna. The equipment will be supporting the orbital tour operation from May 1996 to December 1997, during which Galileo will repeatedly encounter the Jovian satellites Ganymede, Callisto, and Europa. Among the benefits the DGT offers, compared to other telemetry subsystems currently available in the Deep Space Network, are

(1) A capability to record samples of the telemetry signal for later reprocessing over troublesome data gaps, thus enhancing the data return.

(2) A capability to perform full-spectrum combining. Full-spectrum combining refers to combining the telemetry samples from multiple antennas prior to carrier, subcarrier, and symbol demodulation [1]. In doing so, the signal-to-noise ratio (SNR) in the receiver tracking loops is enhanced. This results in either a smaller telemetry loss or the ability to track the signal at a lower signal level.

(3) An increase in coding gain with the use of concatenated (14,1/4) convolutional and four-level redundancy Reed–Solomon codes [2].

(4) A capability to track signals with suppressed carrier, allowing all, instead of partial, signal energy to be put into telemetry data.

The demonstration was planned with the following objectives in mind: (1) to verify the tracking and telemetry processing capability of the DGT with the actual spacecraft, (2) to verify that tracking at small bandwidths, in the order of a milli-Hertz, is feasible, and (3) to verify arraying capability.

This article presents the results of the DOY 062 demonstration, which took place at Goldstone, using the 70-m and 34-m high-efficiency (HEF) antennas. The analysis will focus on system performance in terms of signal-to-noise ratio (SNR) degradation, acquisition delay, and the supportable tracking bandwidths. The array gain will also be considered. In addition, the analysis will extend to studying the characteristics of the Galileo signal, such as its frequency stability and the spacecraft transmitted power. The effect of antenna gain variation due to spacecraft motion on the observed symbol error rate will also be examined.

Section II provides a brief description of the test configuration, both for the ground and aboard the spacecraft. Section III presents the data analysis. A summary is given in Section IV.

II. Configuration

Description of the test configuration is divided into two segments: on the ground and aboard the spacecraft. Deficiencies in the test configuration that prevent a full verification of the capabilities needed for actual support in the 1996 era are also pointed out.

A. Spacecraft Configuration

The Galileo spacecraft was configured in a memory-readout (MRO) mode so that known data could be used as a reference to validate the performance of the ground equipment. Data segments of 640 bits each were extracted from the Attitude and Articulation Control System (AACS) memory and packed into an 800-bit frame, along with a header and real-time engineering data. For a given frame, there were 88 unknown bits associated with real-time engineering data. The remaining 712-bit data segment was known and its equivalent representation in the symbol domain was used in the correlation of the received data stream.[1]

The test was conducted with two data rates available at the time of demonstration: 10 bits/sec with the NASA standard (7,1/2) convolutional code and 40 bits/sec uncoded. This configuration allowed the DGT to be tested at different data rates. In future operation during the orbital tour, it is expected that a rate change will occur several times during the track to take advantage of the improved link margin occurring at high elevation. There are two differences in the data flow in the current configuration, compared to that in the 1996 era:[2]

---

[1] S. Shambayati, "Day 62 DGT Demo Symbol Error Rate Results," JPL Interoffice Memorandum 3393-94-5501 (internal document), Jet Propulsion Laboratory, Pasadena, California, May 26, 1994.

[2] These two characteristics will be removed in future operations with the upload of new flight software in March through May 1996. Under the new configuration, data flow will remain in one path via the buffered memory.

(1) The symbol stream data path was broken whenever the data rate was toggled between 10 and 40 bits/sec.[3] As indicated in Fig. 1, the memory-readout data could come either from the buffered memory during 10 bits/sec or from the low-level memory during 40 bits/sec. A switch in front of the subcarrier modulator helped to select the appropriate input. At the time of change in data rate, the switching likely caused a loss of lock in the receiver on the ground.

(2) The transmitted data sequence to be used as reference for the measurement of symbol error rates was different between the two data rates. This point is illustrated in Fig. 2. The memory data were clocked out at a rate of 8 bits/sec. By the time header information and real-time data were included, the readout was equivalent to 10 bits/sec. At 10 bits/sec, each AACS frame was encoded by the (7,1/2) encoder and became twice as large. At 40 bits/sec transmission, each AACS frame was repeated four times. This exception caused an increase in the complexity of the analysis program that computed symbol error rate (SER).

The spacecraft was configured such that the received signal would emulate as much as possible the levels expected in the orbital tour. The low-power transmitter, which is supposedly 4.8 dB lower than the standard transmitter, was used to reduce the signal level. The spacecraft transmitted data with both residual and fully suppressed carrier modulation. Suppressed-carrier modulation (i.e., 90-deg modulation index) was used at 40 bits/sec. At the lower data rate of 10 bits/sec, the carrier modulation was switched to residual. The modulation index was set at 46 deg (closest to the ideal 45 deg) to maintain a relatively constant symbol SNR level across the data-rate change. Under this residual carrier modulation, the DGT could still emulate the suppressed-carrier tracking mode by ignoring the carrier component. This data set can also be used to isolate any failure associated with suppressed-carrier tracking.

B. Ground Configuration

Before getting into the description of ground configuration, a brief digression to the general architecture of the DGT is needed. A complete DGT configuration, such as the one to be deployed in Canberra in 1996, is depicted in Fig. 3. The DGT consists of two channels: one based on a Block V Receiver (BVR) and the other based on a Full Spectrum Recorder (FSR). Telemetry processing, up to the decoder output, is done independently by each channel. The parallel architecture of the system reduces the risk of equipment failure, thus increasing the data return.[4] This article focuses specifically on the FSR channel.

In the FSR channel, the FSR directly processes the analog 295-MHz signal from the very long baseline interferometry (VLBI)/Radio Science Downconverter (VRD). First, the signal is downconverted to 64 MHz, 8-bit sampled at 256 MHz, then further digitally downconverted to 16 MHz. The samples are time delayed for the purpose of arraying. Individual harmonic components of the square subcarrier, up to the 7th harmonic, are extracted and written to data files on disk for the next assembly to use. The minimal sampling rate of the final product is set to be at least 10 samples per symbol to minimize telemetry processing loss. The Full Spectrum Combiner (FSC) corrects for the frequency and phase difference among different data streams and combines them. The Buffered Telemetry Demodulator (BTD) then performs the carrier and subcarrier demodulation, and symbol extraction on the samples from the FSC or the FSR, in the case of nonarraying. The resulting symbols are decoded in the Feedback Concatenated Decoder (FCD). If both FSR and BVR channels are used, the two FCD outputs are merged and the best product is delivered to the Project.

---

[3] "Module GLL-3-280, Functional Requirement Galileo Orbiter Telemetry Measurements and Data Formats," *Galileo Orbiter Functional Requirements*, Galileo Project Document 625-205 (internal document), Jet Propulsion Laboratory, Pasadena, California, p. 13, January 13, 1986.

[4] A more detailed description can be found in T. Pham, *DSCC Galileo Telemetry Subsystem, Functional Design and Software Requirements Document*, TDA/DSN Document 834-43, JPL D-11226 (internal document), Jet Propulsion Laboratory, Pasadena, California, December 21, 1993.

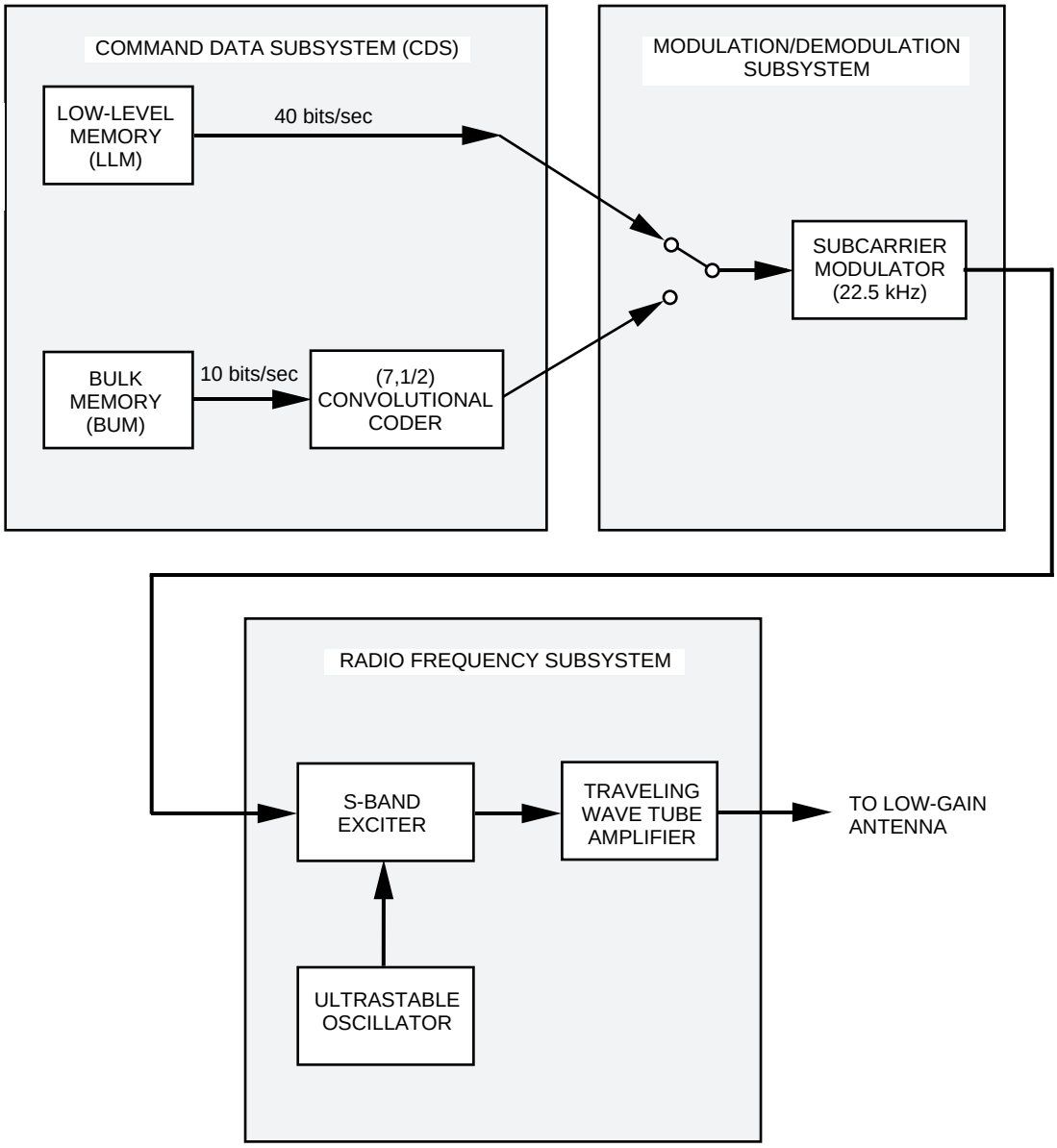

Fig. 1. Data flow onboard the Galileo spacecraft.

Figure 4 presents the DSN ground configuration on DOY 062. The Galileo signal was received at the 70-m (DSS-14) and 34-m HEF (DSS-15) antennas. Even with the use of the low-power transmitter, the Galileo signal level was in the range of 0- to 1-dB symbol SNR, which was still significantly higher than the expected future operating level of −5 dB.[5] To simulate a lower SNR level, additional noise from the noise diode in the Microwave Precision Power Monitor (PPM) assembly was continuously injected into the low-noise amplifier (LNA) input at DSS 14. Different noise levels were added at different times to emulate different SNR conditions. The amplified S-band (2.3-GHz) signals were converted to 295 MHz IF by the VRD. The IF Distribution Assembly then distributed the signals to the FSRs. The FSR samples

[5] This −5-dB level corresponds to the SNR threshold of the new concatenated (14,1/4) convolutional and four-level redundancy Reed–Solomon codes for which the decoded bit error rate is less than 10^{-7}. The operational strategy planned for the orbital tour dictates that the symbol SNR level be kept constant at the decoder threshold. The data rate is adjusted accordingly, based on the power availability in the link budget, to maximize the data return.

were stored on tapes and brought back to JPL for further processing in the FSC and BTD. Once properly demodulated, the BTD symbols were compared against the reference data stream and the symbol error rates were generated. Detailed description on the symbol-error-rate analysis can be found in Footnote 1. Note that the demodulated symbols from the BTD were not processed through the FCD. The reasons were that the low signal level would have resulted in a high bit error rate, in the vicinity of 50 percent for the (7,1/2) convolutional code, and that the (7,1/2) code is not going to be used in normal operations during the orbital tour.

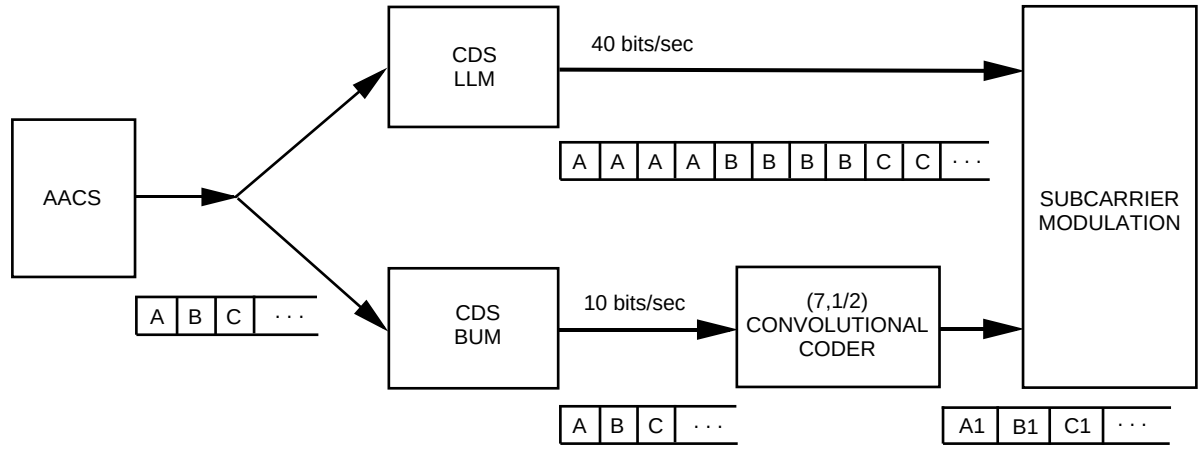

Fig. 2. Data sequence of 10 and 40 bits/sec.

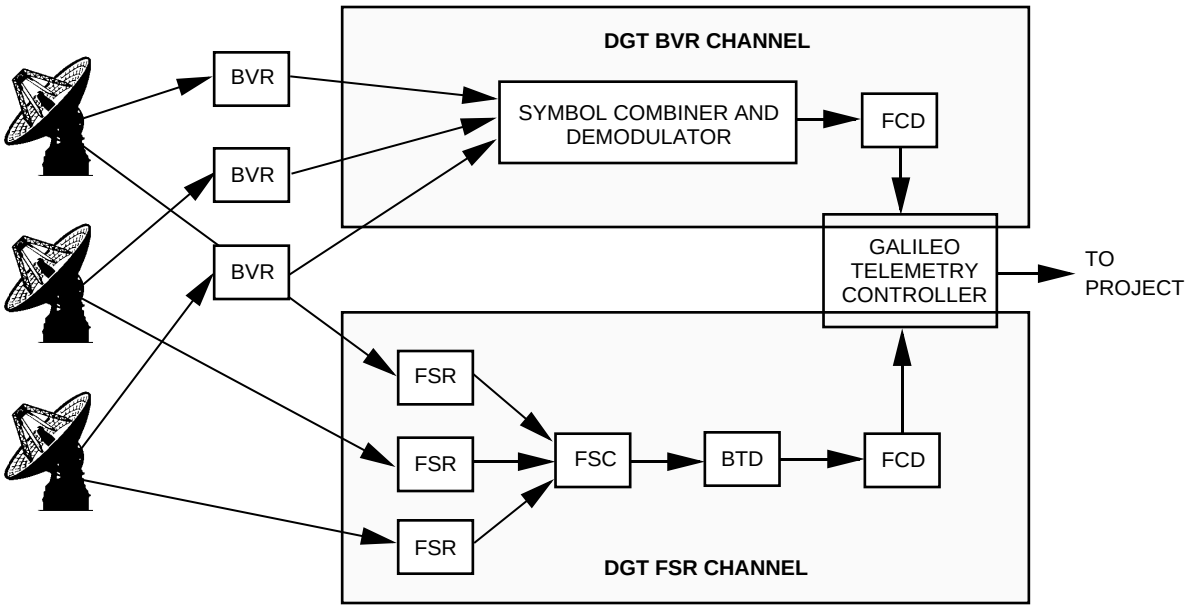

Fig. 3. DGT architecture.

Also indicated in Fig. 4 are monitor data provided at different stages of processing. The FSRs and FSC reported the data power–to–noise spectral density ratio (P_d/N_o) using the fast Fourier transform (FFT). These measurements were translated to symbol SNR (E_s/N_o) using the predicted data rate for an easy and consistent comparison with the BTD estimation. The BTD provided symbol SNR (E_s/N_o). The analysis program produced measured symbol error rates, which were available only over the memory readout period.

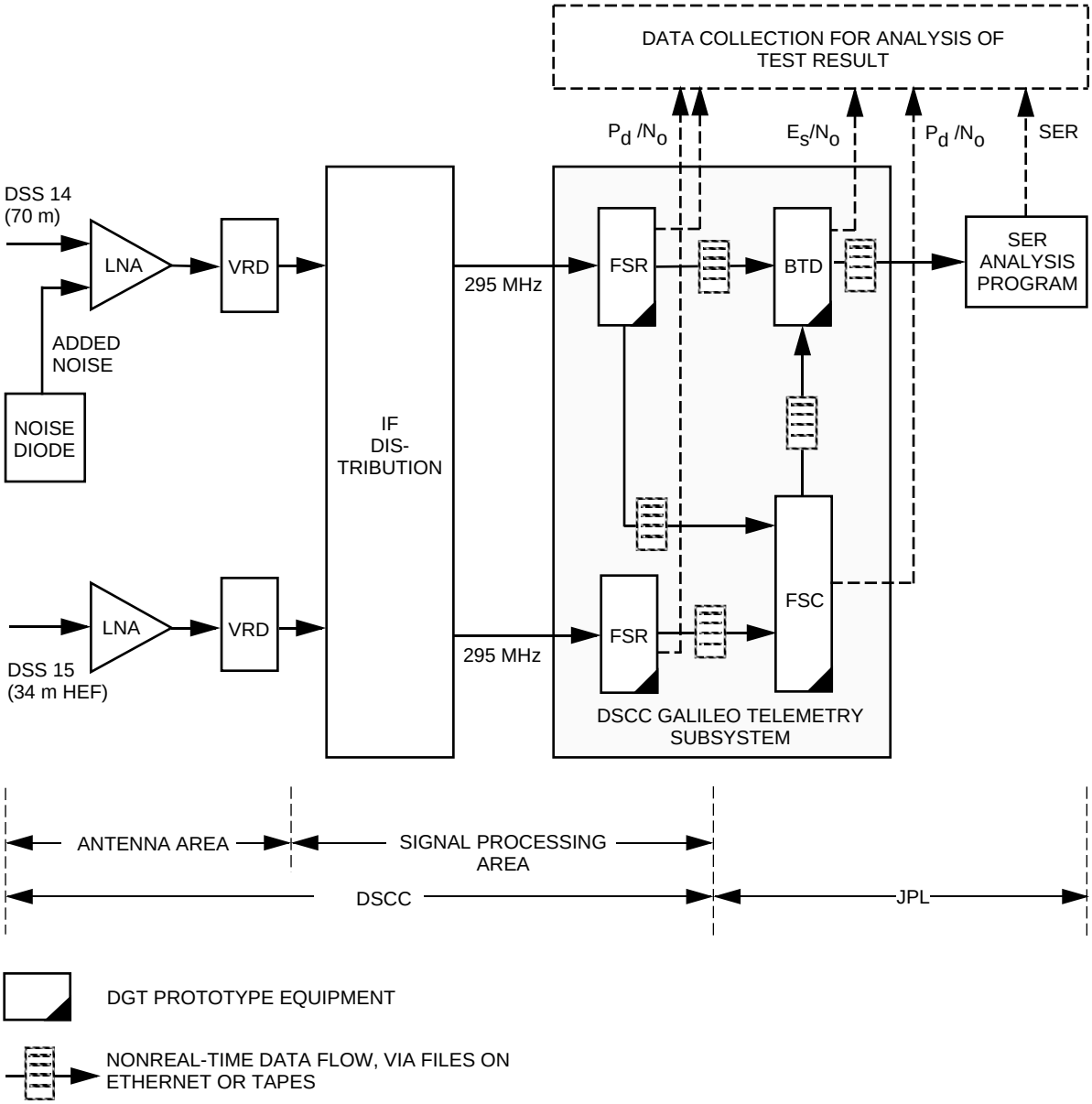

Fig. 4. Test configuration in the DSN.

C. Operational Timeline

Figure 5 presents the operational timeline events on the DOY 062 track. On the spacecraft side, there are four different configurations. The two outer configurations (involving the beginning and end of the track) were of standard operations, for the purpose of performance verification prior to and after the test. The two inner configurations involved memory readout and were the focus of the test. On the ground, noise injection was done in four stages: none at the beginning and at the end of the track, 8-K noise added from 10:49 to 13:16 Greenwich mean time (GMT), and 46-K noise added from 13:16 to 14:35 GMT. This resulted in three nominal signal conditions with symbol SNRs of about 0.5 dB, −0.5 dB, and −4.2 dB over the memory readout region.[6] (Near the end of the track, a 7.3-dB level was also available

[6] These levels are referenced to the FSR input or, equivalently, the antenna input. They include power from all subcarrier harmonics.

when the spacecraft was reconfigured for normal operation with the high-power transmitter). To properly track the signal, the receiver bandwidths in the BTD were set such that at least 15-dB-Hz loop SNRs were ensured. Most of the track was done with 0.25-Hz carrier, 0.09-Hz subcarrier, and 0.01-Hz symbol bandwidths. During the period where symbol SNR dropped to −4.7 dB-Hz (from 13:16 to 14:35 GMT), a set of narrower loop bandwidths (0.05 Hz for carrier, 0.02 Hz for subcarrier, and 0.003 Hz for symbol) was used. The FSR configuration also varied during the track. The prototype FSR was limited to capturing two spectral components of the signal, either the two subcarrier harmonics (1st and 3rd) or only the 1st harmonic and the carrier. Residual carrier data, from 11:11 to 12:14 GMT, were used for the validation purpose. Over this period, the SNR in telemetry data dropped by 0.46 dB. As the FSR switched in (at 11:03 GMT) and out (at 12:14 GMT) of the carrier-capturing mode, an approximate 9-min data outage occurred as a result of reconfiguration.

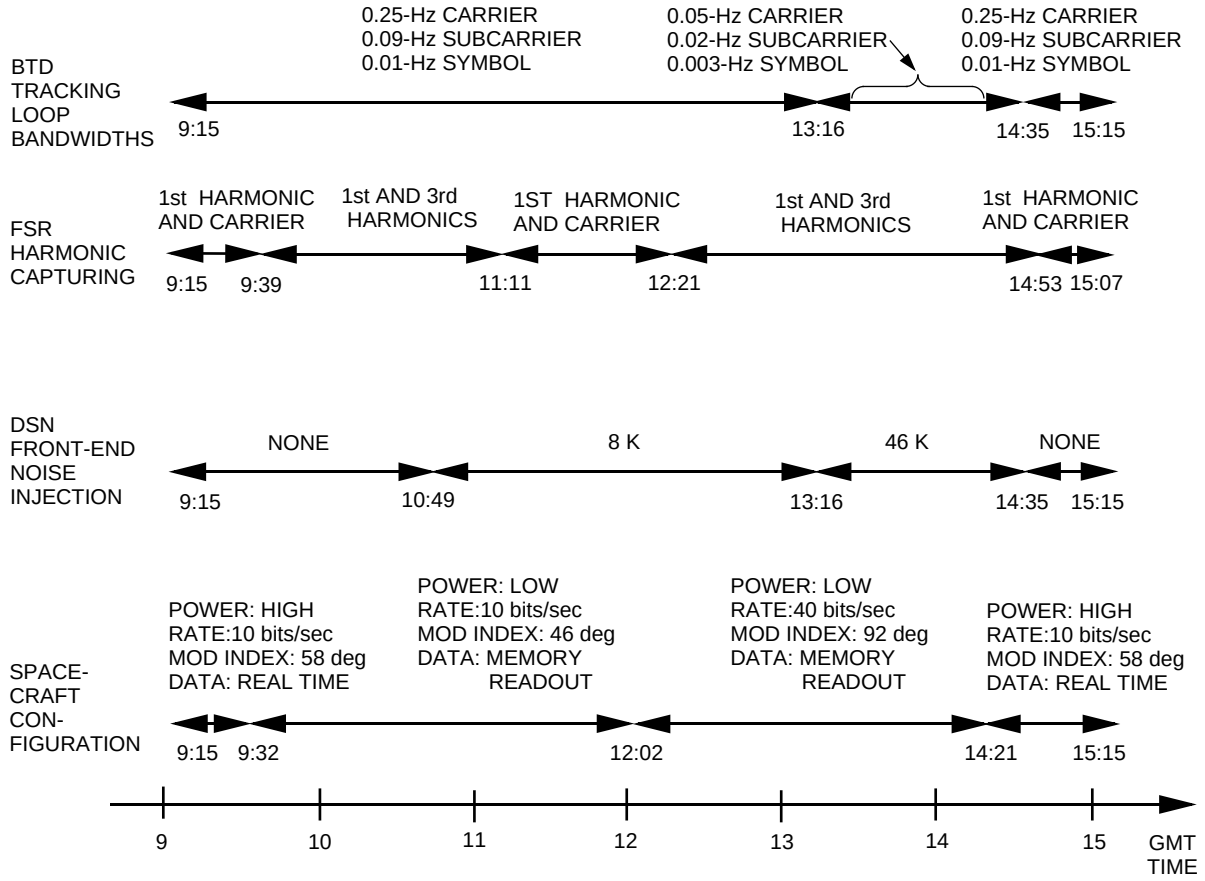

Fig. 5. Timeline events on spacecraft and DSN configuration.

III. Data Analysis

In this section, we focus on performance of the system. Particular attention is given to the SNR degradation and array improvement, acquisition time, the existence of data gaps caused by abrupt changes in signal conditions, and the feasibility of tracking at a small bandwidth. Also examined is the stability of the carrier and subcarrier frequencies. Any differences, if they existed, between the expected and observed signal characteristics will also be pointed out.

Predicted symbol SNR was obtained from the Galileo S-Band Analysis Program (GSAP).[7] The antenna-referenced predicts were then translated to such observables as FSR, FSC, and BTD outputs using the degradation model presented in Fig. 6. In this model, the expected SNR degradation in the FSR was 0.99 dB for the 1st-harmonic capture and 0.53 dB for the 1st- and 3rd-harmonic captures. This degradation included the outer harmonic loss and the 0.08-dB degradation due to filter mismatch. For the FSC, the gain was expected to be equal to the theoretical gain minus a 0.1-dB loss due to thermal jitters. In the BTD, the expected degradation was 0.1 dB above the theoretical loss in the carrier, subcarrier, and symbol tracking loops. The theoretical loss in the BTD was a function of the symbol SNR, symbol rate, and tracking loop bandwidths. The extra 0.1 dB accounted for any filter mismatch.

The observed and predicted performances seen at different points in the system are shown in Figs. 7, 8, and 9. Figure 7 focuses on the symbol SNR observed at the FSR and BTD output under the single antenna condition (DSS 14 only). Figure 8 illustrates the array gain referenced to DSS 14. The symbol SNRs observed at DSS 14 and the combined symbol SNRs at DSS 14 and DSS 15 are shown. A 1-min integration window for symbol SNR estimation was used in Figs. 7 and 8. Figure 9 presents the symbol error rate for the single-antenna configuration. Each SER report corresponds to one AACS frame. That is, the integration windows for the correlation between the reference and received data were 1600 symbols at a 10 bits/sec data rate, and 3200 symbols at 40 bits/sec. Several conclusions can be drawn from these charts.

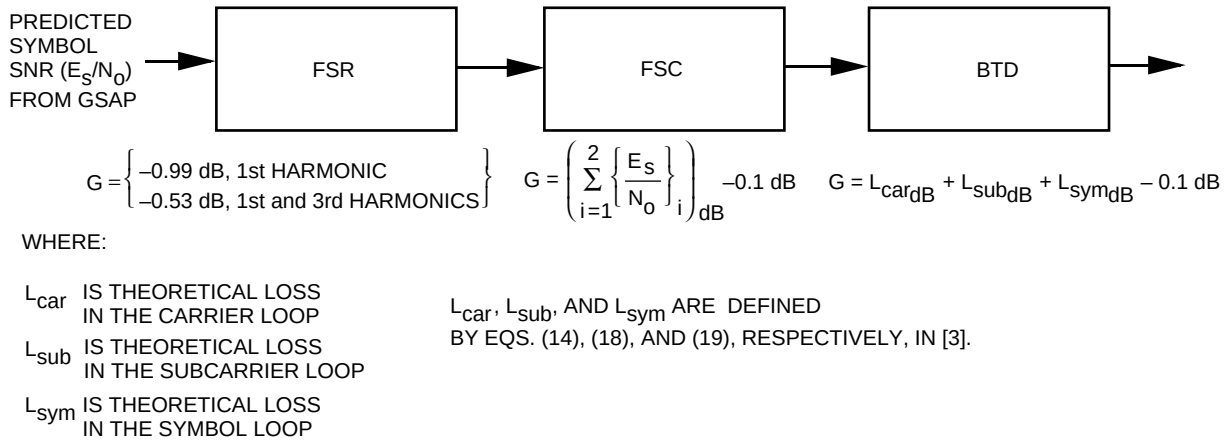

Fig. 6. Model of gain/loss profile in the DGT.

A. Predicts Versus Measurement

In Fig. 7, the given predicts were referenced to the FSR and BTD outputs. The predicted loss in the BTD, i.e., the difference between the predicted FSR and BTD symbol SNRs, was influenced by three factors: (1) setting of tracking loop bandwidths, (2) input symbol SNR, which was a function of the number of captured harmonics, noise injection on the ground, and selection of the high- or low-power transmitter onboard the spacecraft, and (3) the data rate.

Both the FSR and FSC estimated the SNR based on FFT spectral analysis of the cross product of the upper and lower sideband of the first subcarrier harmonic.[8] The BTD, on the other hand, estimated

[7] D. Bell, "Summary of Final Updates to GSAP 3.5 to Create GSAP 3.6," JPL Interoffice Memorandum 3392-94-087 (internal document), Jet Propulsion Laboratory, Pasadena, California, August 10, 1994.

[8] D. Rogstad, "Processing in the Full Spectrum Recorder and the Full Spectrum Combiner," personal communication through unpublished notes, Tracking Systems and Applications Section, Jet Propulsion Laboratory, Pasadena, California, 1993.

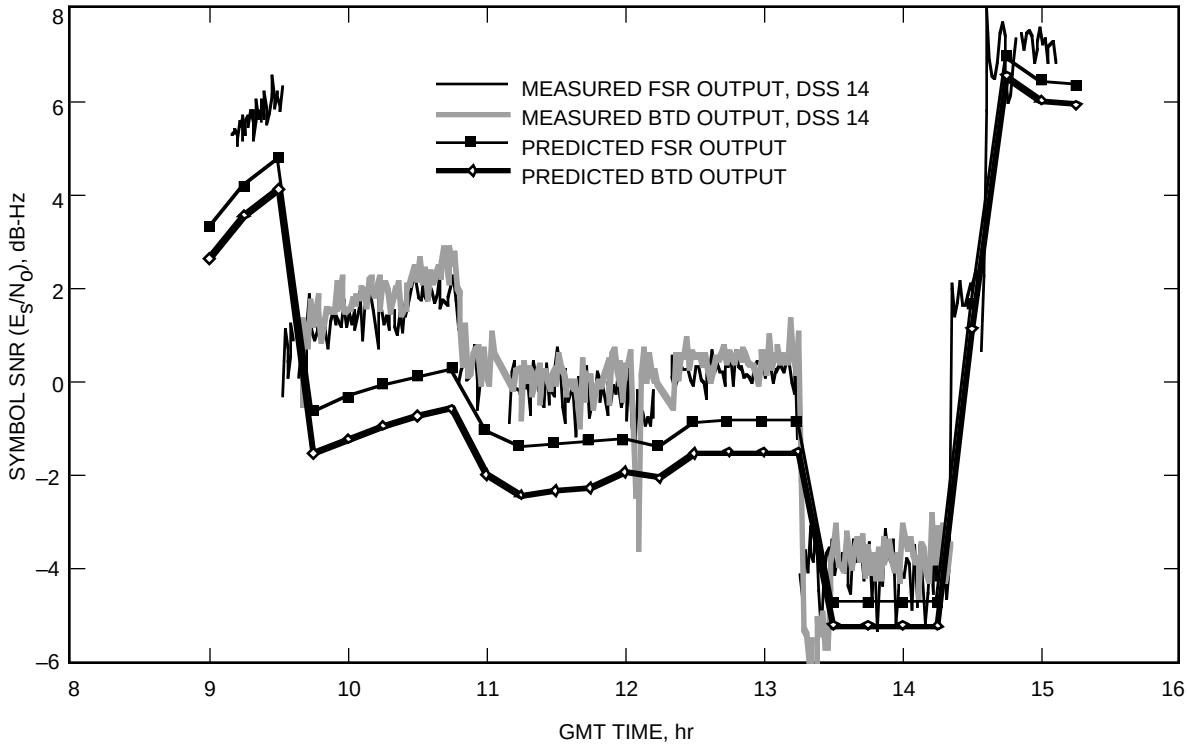

Fig. 7. Result from FSR and BTD, single antenna (DSS 14), DOY 062, 1994.

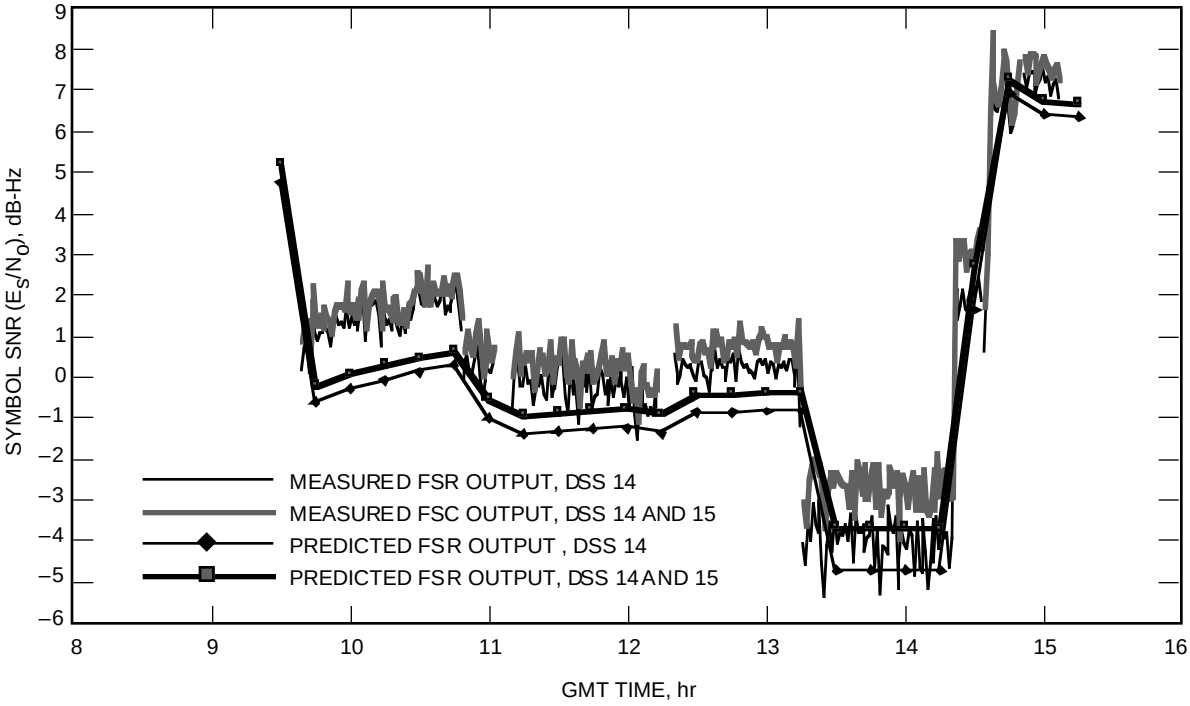

Fig. 8. Illustration of arraying gain, DOY 062, 1994.

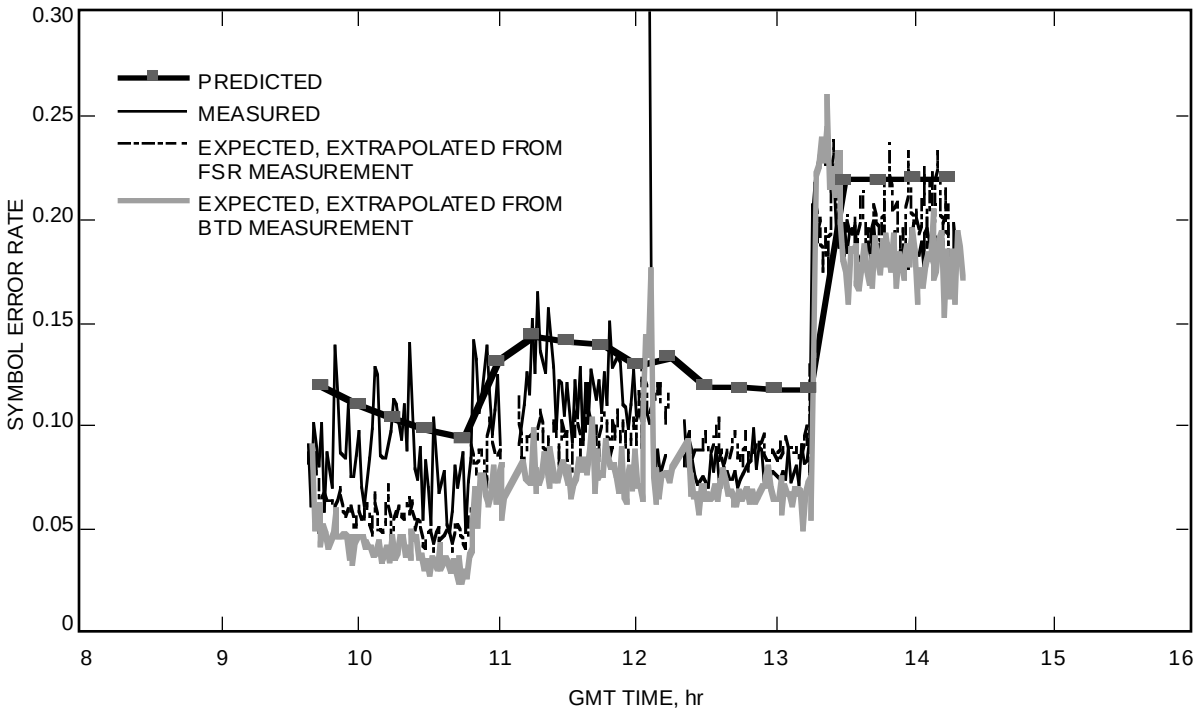

Fig. 9. Symbol error rate at DSS 14, DOY 062, 1994.

symbol SNR (E_s/N_o) using the split-symbol-moment-estimation (SSME) algorithm [4]. The two symbol SNR profiles from the FSR and BTD closely follow each other. This agreement established a general consistency between the two estimations. However, the measured SNRs from the BTD were about 0.3 dB higher than those from the FSR, instead of 0.6 to 0.9 dB lower. This difference is being sorted out and correction will be made prior to the DGT formal delivery to DSN Operations.

The SERs determined by the SER Analysis Program, shown in Fig. 9, were in the approximated region of the reported signal level. This fact lends support to the belief that the DGT was operating properly. The SER profile was essentially an inversion of the symbol SNR profile. Also indicated in Fig. 9 are the expected SERs based on the symbol SNRs reported by the BTD and FSR (with proper accounting of BTD loss). During the 40-bit/sec period, the measured SERs lie between the BTD and FSR measurements. During the 10-bit/sec period, the measured SERs appeared to be high and had a large variation. This problem is being further investigated.

When the predicts and measurements were compared, the observed SNRs were found to be much higher. The positive residual was attributed to an error in the GSAP prediction. Specifically, GSAP used prelaunch calibration data in computing the antenna gain as a function of cone angle. This calculation was about 1 dB lower than that experienced inside the 10-deg cone angle. Subsequently, the GSAP's database was updated to remove this discrepancy.[9]

The residuals also varied over time, as seen in Table 1. Three sets of residuals are presented, from the FSR, BTD, and SER measurements. At the beginning of the track, the residual SNRs were as large as 2.0 dB. Toward the end of the track, they progressively reduced to 1.0 dB. Since there was no noise injection at the start of the track, one might suspect that the variation was related to the added noise. That is, contribution of the added noise, which was measured during the precalibration period, was

[9] D. Bell, op. cit.

perhaps overestimated. However, this was ruled out due to the fact that the residual remained small at the end of the track when all added noise was removed, i.e., post 14:35 GMT. It is not known at this point what caused this phenomenon.

Table 1. Residual symbol SNR, observed at the FSR and BTD.

Configuration	Residual symbol SNR, dB (measured−predicted)		
	FSR	BTD	SER
From 9:39 to 10:49 GMT (low-power transmitter, 10 bits/sec, no added noise)	1.9	2.9	0.7
From 10:49 to 12:02 GMT (low-power transmitter, 10 bits/sec, 8-K noise added)	1.5	2.3	0.6
From 12:02 to 13:16 GMT (low-power transmitter, 40 bits/sec, 8-K noise added)	1.2	2.0	1.6
From 13:16 to 14:21 GMT (low-power transmitter, 40 bits/sec, 46-K noise added)	1.0	1.8	1.2
From 14:37 to 15:06 GMT (high-power transmitter, 10 bits/sec, no noise added)	1.1	–[a]	–[a]

[a] Not available.

B. Acquisition Time in the BTD

The acquisition in the BTD, at the time of the demonstration, was limited to carrier-phase and subcarrier-phase acquisitions. A determination of frequency offsets was done off-line, either via self-determination or via FSR detection. Phase acquisition in the BTD was found to be less than 1 min. The in-lock time was defined as that time when the estimated symbol SNRs first achieved stability.

During the track, the BTD was subjected to three disruptions. The first occurred at 11:13 GMT with the introduction of the 8-K noise diode, which resulted in a 1.2-dB drop in symbol SNR. The second was caused by a data-rate transition from 10 to 40 bits/sec at 12:02 GMT. The last took place at 13:15 GMT when the 46-K noise diode was injected into the system. Due to a significant change in the symbol SNR of 3.7 dB, the BTD overreacted in the last event and took longer to recover. The recovery times associated with the three disruptions were 4, 5, and 14 min, respectively. Is this a point of concern? Before answering this question, let us take a look at what is expected in future operations. As previously mentioned in Section II, the data path will not be disrupted by rate changes. So, the disruption associated with the rate change is not a point of concern. The impact of the SNR change in the first and third disruptions, however, may be problematic. The expected distribution of data-rate changes results in a 0.97- to 1.8-dB change in the SNR for 74 percent of the time of the entire orbital tour, a 3.0-dB change for 25 percent of the time, and a 4.2- to 4.7-dB change for 1 percent of the time.[10] These levels of change are not much different from the test conditions. Therefore, more consideration will need to be given to this area to ensure proper operations during actual mission support.

[10] These values are based on A. DiCicco, "Distribution of Galileo Data Rate Changes," JPL Interoffice Memorandum GLL-MOT-94-092 (internal document), Jet Propulsion Laboratory, Pasadena, California, May 10, 1994.

One might also notice that there were two empty data segments. They occurred between 11:02 and 11:11 GMT, and 12:13 and 12:21 GMT. These gaps were the results of FSR configuration changes in the number of subcarrier harmonics to be captured.

C. Tracking With Small Loop Bandwidths

For the receiver to properly track the phase of the incoming signal, the loop SNR must be at least 15 dB-Hz. This requirement translates to a reduction in the loop bandwidth as the signal received from the spacecraft becomes weaker and weaker. In addition, the narrower the loop, the less phase jitter and, thus, less degradation. For the Galileo mission, this means more link margin. There is another way of looking at this: With smaller loop bandwidth, the loop SNR exceeding the 15-dB threshold can be realized more quickly. This advantage in turn enables successful tracking at lower elevation, thus lengthening the tracking time. However, the loop can be narrowed only to the point where the frequency instability of the signal becomes a problem.

The minimum bandwidths currently available in the DSN telemetry systems are 1 Hz for the carrier, 30 mHz for the subcarrier, and 30 mHz for the symbol. The result from this demonstration indicates that a tracking bandwidth of 0.25 Hz to 50 mHz for the carrier, 20 mHz to 10 mHz for the subcarrier, and 10 mHz to 3 mHz for the symbol are supportable. For example, by narrowing these bandwidths to 0.1 Hz for the carrier, 10 mHz for the subcarrier, and 5 mHz for the symbol, the signal can be tracked at an SNR at least 8 dB lower and with a degradation of 0.8 dB less, assuming the configuration of a fully suppressed carrier, a 40-symbol/sec data rate, and a −4.7-dB symbol SNR.

D. Array Performance

Figure 8 shows the measured and predicted array gain in the FSC. Without any noise in the front end, the predicted SNR level at DSS 15 was about 9.5 dB below that at DSS 14. The predicted gain for this configuration was 0.38 dB. As additional noise was injected into the system, the SNR level at DSS 14 got smaller, and the relative contribution from the DSS 15 antenna became more pronounced. The predicted gain increased to 0.47 dB during a period of 8-K added noise, and 1.06 dB during the 46-K noise-injection period.

Table 2 summarizes both the measured and predicted average gain for each of the main configurations. The result indicates that the arraying gain was fully realized. Notice that during the period of the 46-K noise injection, the measured gain of 1.33 dB was much higher than the predicted gain of 1.06 dB. This discrepancy is believed to be an artifact, due to the fact that the low signal level at the single antenna (DSS 14) resulted in erroneous measurements. These inaccurate measurements corresponded to large variation that often fell below the −5-dB level seen in Fig. 8.

Table 2. Array performance.

Configuration	Array gain, dB	
	Predicted	Measured
From 9:39 to 10:49 GMT (no added noise)	0.38	0.34
From 10:49 to 13:16 GMT (8-K noise added)	0.47	0.54
From 13:16 to 14:35 GMT (46-K noise added)	1.06	1.33
From 14:35 to 15:06 GMT (no added noise)	0.34	0.36

E. Observed Spacecraft Signal Characteristics

The carrier and subcarrier frequency detected by the FSR appeared to be stable. The carrier residual frequency varied from 0.82 to 0.94 Hz. The subcarrier frequency was found to be 0.3 Hz below the expected 22.5 kHz. Its variation ranged from 0.34 to 0.32 Hz. This stability performance was consistent with the fact that the BTD was able to maintain tracking at a small bandwidth, as discussed earlier.

The effect of antenna gain variation on the observed symbol error was also examined. This variation was due to the 3 rotations/min of the spacecraft. Because there were unknown real-time data imbedded in the received telemetry frames, special care was given to the spectral analysis of the SER. Instead of applying an FFT directly on the whole measured SER data set, FFT processing on individual frames was needed. Over the 712-bit known data segment, 16 SER calculations were performed with an integration of roughly 44 symbols. The 16 samples were FFT transformed. Then an average FFT was computed over several frames. The final result was plotted in Fig. 10. The result demonstrated a clear tone at 0.05 Hz (a 20-sec period or 3 rotations/min) and 0.1 Hz (10-sec period). The detection of a faster oscillation with a 10-sec period was consistent with an earlier finding.[11] These oscillations in the SER confirmed the need to have a link margin sufficient to meet the overall bit error–rate requirement.

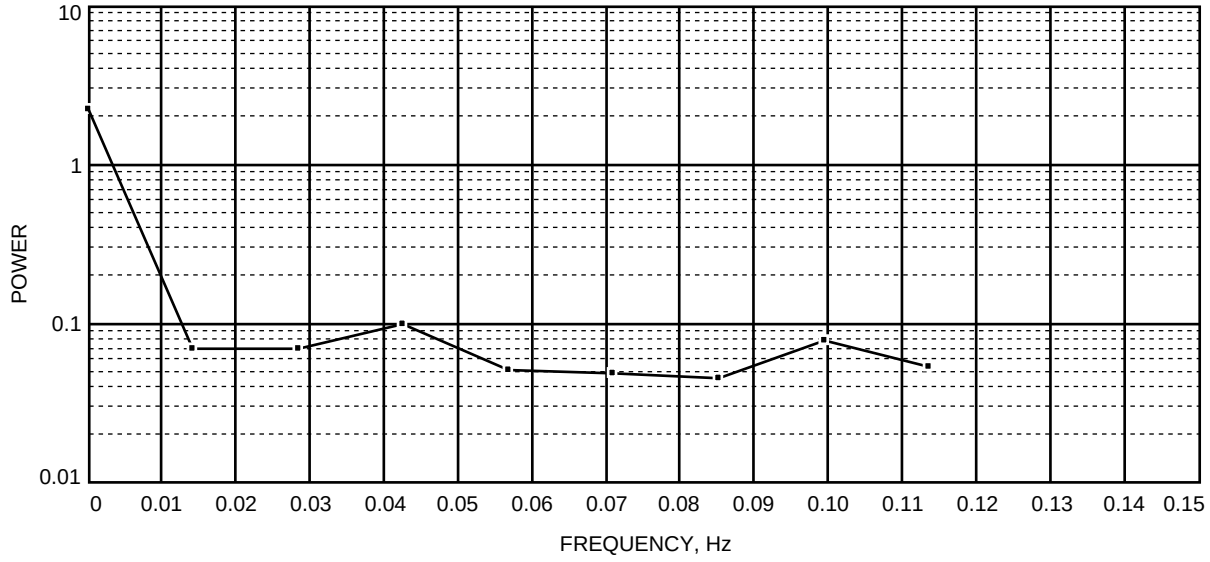

Fig. 10. Power spectral density of symbol error rate, DOY 062, 1994.

An abnormality related to the spacecraft transition from the high- to the low-power transmitter was detected. The two transitions occurred at 9:32 GMT, from high to low, and at 14:21 GMT, from low to high. Table 3 presents the expected and observed SNR changes for each transition. It was found that the measured change for both transitions was 0.6 dB less than expected. Notice that in conjunction with the power change, there was also a change in the modulation index and a data-rate change; however, these factors, as discussed next, were not responsible for the discrepancy. First, notice that a change in data rate was not common at both transitions; rather it occurred only at the second transition. This and the fact that good symbol synchronization was achieved at the specified data rate indicate that the data rates were well known and that the data-rate change was not the cause of the problem. Second, the uncertainty associated with the actual setting of the modulation indexes was found to be quite small, within the accuracy of the measurement. The modulation indexes extracted from the FSR measurement

[11] D. Watola, "DOY 173/124 Galileo LGA Downlink Data Analysis," JPL Interoffice Memorandum 331-93.5-030 (internal document), Jet Propulsion Laboratory, Pasadena, California, October 20, 1993.

of relative power in the carrier and data components were within 2 deg of the expected values. For instance, the measurement indicated a modulation index of 59.7 deg versus 58 deg expected, 47.3 deg versus 46 deg expected, and 59.9 deg versus 58 deg expected, over the three periods of 9:15 to 9:30 GMT, 11:11 to 12:02 GMT, and 14:53 to 15:07 GMT, respectively. This agreement between observed and expected modulation indexes eliminated the uncertainty in the modulation index setting from the list of possible suspects. As a result, the discrepancy between the expected and observed change in the power levels across the transition were likely a result of switching between the low-power and high-power transmitters. The gain difference between the two transmitters was only 4.2 dB instead of the expected 4.8 dB.

Table 3. Discrepancy in SNR as the spacecraft transitions between normal and test configurations.

Configuration	Performance, dB	
	Predicted	Measured
First transition (mod index: 58 → 46 deg; power: P → P − 4.8 dB)	−6.23	−5.6
Second transition (mod index: 92 → 58 deg; power: P → P + 4.8 dB data rate: 40 bits/sec uncoded → 10 bits/sec coded)	6.38	5.8

IV. Conclusion

In conclusion, the demonstration has shown that the functions that are required for future Galileo support were realized in the DGT prototype. Proper data sampling of selected harmonics in the FSR, suppressed-carrier tracking in the BTD, and the ability to track at milli-Hertz bandwidths were demonstrated. The observed SNR degradation in the subsystem was found to be reasonable, with the inconsistency in the reported measurements from the FSR and BTD noted. Full spectrum combining was carried out with a measured gain within 0.1 dB of the expected.

In addition, it was discovered that the transition from the high-power to the low-power transmitter did not result in an expected power change. The difference between the measured and expected change was 0.6 dB. The impact of the gain variation on the received signal due to spacecraft rotation was observed as an oscillation in the measured symbol error rate. Although the measurement was made with essentially uncoded symbols, there should be some impact on the output of the future (14,1/4) convolutional and Reed–Solomon codes. The confirmation of this oscillation lends support to the conservative approach that the Galileo S-Band Analysis Program is taking, in terms of reserving some link margin to compensate for this effect.

The demonstration also pointed to a large discrepancy between predicts and measurements. This knowledge helped to update the prediction model accordingly, resulting in better mission operation planning.

Acknowledgments

This analysis would not have been possible without the dedication and support of many people. We would like to express our sincere thanks to Roger Lee, Dave

Fort, Kay Cloud, and Andre Jongling for staying up all night supporting the DOY 062 track. Obviously, data collection would not have been realized without extensive development effort from the FSR team led by Dave Rogstad and including Elliott Sigman, D'Arcy Tyrell, Maria Carlton, Ron Baalke, Robert Navarro, Robert Proctor, Leslie White, and Ismael Cruz. Our gratitude is also directed to Robert Lee, who spent many hours helping with the data processing, and to other BTD members, namely, Sami Hinedi, Kimberly Simpson, Haiping Tsou, Biren Shah, Tim Dry, and Simpson Million, who are supporting the BTD development. A contribution from Robert Kahn and Jeff Piero in prototyping the FSC and processing the combined data was valuable in determining the array performance. Excellent DSN operations support from Larry Bracamonte with noise injection, Glyn Martinez with the hardware installation, John Rothrock with predicts generation, and Michelle Andrews with general network operation support was greatly appreciated. Thanks to Richard Benninger for facilitating the equipment installation at the DSCC and to Joseph Statman, the Task Manager, for planning the demonstration and providing all necessary support to make it happen. We also would like to acknowledge the support from the Galileo Project in accommodating our requested test configuration, notably Eileen Theilig, Vickere Blackwell, Leif Harke, and Dave Allestad. And last but not least, our thanks to Steve Townes for generously agreeing to referee this article despite his schedule constraint and for many good writing suggestions.

References

[1] D. Rogstad, "Suppressed Carrier Full-Spectrum Combining," *The Telecommunications and Data Acquisition Progress Report 42-107, vol. July–September 1991*, Jet Propulsion Laboratory, Pasadena, California, pp. 12–20, November 15, 1991.

[2] S. Dolinar and M. Belongie, "Enhanced Decoding for the Galileo S-Band Mission," *The Telecommunications and Data Acquisition Progress Report 42-114, vol. April–June 1993*, Jet Propulsion Laboratory, Pasadena, California, pp. 96–111, August 15, 1994.

[3] A. Mileant and S. Hinedi, "Overview of Arraying Techniques in the Deep Space Network," *The Telecommunications and Data Acquisition Progress Report 42-104, vol. October–December 1990*, Jet Propulsion Laboratory, Pasadena, California, pp. 109–139, February 15, 1991.

[4] B. Shah and S. Hinedi, "Performance of the Split-Symbol Moments SNR Estimator in the Presence of Inter-Symbol Interference," *The Telecommunications and Data Acquisition Progress Report 42-98, vol. April–June 1989*, Jet Propulsion Laboratory, Pasadena, California, pp. 157–173, August 15, 1989.